Large Impact of the Decay of Niobium Isomers on the Reactor $\bar{\nu}_e$ Summation Calculations

V. Guadilla,[1,*] A. Algora,[1,2,†] J. L. Tain,[1] M. Estienne,[3] M. Fallot,[3] A. A. Sonzogni,[4] J. Agramunt,[1] J. Äystö,[5] J. A. Briz,[3] A. Cucoanes,[3] T. Eronen,[5] L. M. Fraile,[6] E. Ganioğlu,[7] W. Gelletly,[8] D. Gorelov,[5] J. Hakala,[5] A. Jokinen,[5] D. Jordan,[1] A. Kankainen,[5] V. Kolhinen,[5] J. Koponen,[5] M. Lebois,[9] L. Le Meur,[3] T. Martinez,[10] M. Monserrate,[1] A. Montaner-Pizá,[1] I. Moore,[5] E. Nácher,[11,1] S. E. A. Orrigo,[1] H. Penttilä,[5] I. Pohjalainen,[5] A. Porta,[3] J. Reinikainen,[5] M. Reponen,[5] S. Rinta-Antila,[5] B. Rubio,[1] K. Rytkönen,[5] T. Shiba,[3] V. Sonnenschein,[5] E. Valencia,[1] V. Vedia,[6] A. Voss,[5] J. N. Wilson,[9] and A.-A. Zakari-Issoufou[3]

[1]*Instituto de Física Corpuscular, CSIC-Universidad de Valencia, E-46071 Valencia, Spain*
[2]*Institute of Nuclear Research of the Hungarian Academy of Sciences, Debrecen H-4026, Hungary*
[3]*Subatech, IMT-Atlantique, Université de Nantes, CNRS-IN2P3, F-44307 Nantes, France*
[4]*NNDC, Brookhaven National Laboratory, Upton, New York 11973-5000, USA*
[5]*University of Jyväskylä, FIN-40014 Jyväskylä, Finland*
[6]*Universidad Complutense, Grupo de Física Nuclear and UPARCOS, CEI Moncloa, E-28040 Madrid, Spain*
[7]*Department of Physics, Istanbul University, 34134 Istanbul, Turkey*
[8]*Department of Physics, University of Surrey, GU2 7XH Guildford, United Kingdom*
[9]*Institut de Physique Nuclèaire d'Orsay, 91406 Orsay, France*
[10]*Centro de Investigaciones Energéticas Medioambientales y Tecnológicas, E-28040 Madrid, Spain*
[11]*Instituto de Estructura de la Materia, CSIC, E-28006 Madrid, Spain*

(Received 24 September 2018; revised manuscript received 23 November 2018; published 30 January 2019)

Even mass neutron-rich niobium isotopes are among the principal contributors to the reactor antineutrino energy spectrum. They are also among the most challenging to measure due to the refractory nature of niobium, and because they exhibit isomeric states lying very close in energy. The β-intensity distributions of ^{100gs,100m}Nb and ^{102gs,102m}Nb β decays have been determined using the total absorption γ-ray spectroscopy technique. The measurements were performed at the upgraded Ion Guide Isotope Separator On-Line facility at the University of Jyväskylä. Here, the double Penning trap system JYFLTRAP was employed to disentangle the β decay of the isomeric states. The new data obtained in this challenging measurement have a large impact in antineutrino summation calculations. For the first time the discrepancy between the summation model and the reactor antineutrino measurements in the region of the shape distortion has been reduced.

DOI: 10.1103/PhysRevLett.122.042502

Nuclear reactors produce an enormous flux of antineutrinos due to the β decay of the fission fragments. On average six β decays are produced per fission, thus generating six antineutrinos. This is why nuclear reactors have been of particular relevance in neutrino physics since they allowed the discovery of this elusive particle in 1954 by Reines and Cowan [1]. Recently, three reactor antineutrino oscillation experiments have determined the θ_{13} mixing angle with unprecedented precision (Double Chooz [2], Daya Bay [3], and RENO [4]), showing that this mixing angle is not as small as previously assumed, thus opening new possibilities for experiments that could provide information on the mass hierarchy and the charge-parity (CP) violation phase. Future reactor experiments such as JUNO [5] and RENO-50 [6] are aimed at these fundamental goals.

Existing and future reactor antineutrino experiments require the determination of the primary antineutrino spectrum from the reactor. Presently there are two main approaches to determining the spectrum. The standard approach is based on the conversion of integral β-spectra measurements available for the main fissile isotopes in pressurized water reactors (PWR): ^{235}U, ^{239}Pu, ^{241}Pu, and ^{238}U [7,8]. A recent revision of this method [9,10] suggested that there is a deficit of the antineutrino flux in short baseline reactor experiments [11]. This result, known as the reactor antineutrino anomaly, has attracted considerable attention since one of the possible explanations for this deficit is the existence of sterile neutrinos. Recently, the Daya Bay collaboration suggested that uncertainties in our knowledge of the reactor antineutrino flux, affecting in particular ^{235}U, could account for the anomaly [12], but the discussion is still open. In addition to the anomaly, the antineutrino spectra measured by RENO, Daya Bay, and Double Chooz exhibit an excess in the range of 5–7 MeV (colloquially referred to as the "shape distortion" or "bump") with respect to the prediction from the conversion model [13–15], which is not understood. These results

underline the need to improve the predictions of the reactor antineutrino spectrum.

An alternative way of determining the antineutrino spectrum is to perform summation calculations. In this approach the total antineutrino spectrum is computed as the sum of the antineutrino spectra associated with the decay of each fission product weighted by the corresponding activity. The antineutrino spectrum for each decay is constructed using the available β-intensity distributions from nuclear data bases and making assumptions about the shapes of β transitions. Since the summation method depends on the quality of the available data, improvements can be made by measuring unknown β-intensity distributions, as well as providing decay data free from the Pandemonium systematic error [16]. This error is related to the modest efficiency of the HPGe detectors commonly used in high-resolution β-decay experiments. It results in an incorrect determination of the β-intensity distribution due to the nondetection of numerous weak γ rays in the deexcitation of states at high excitation energy in the daughter nucleus.

In the summation approach, identifying the nuclei that are the main contributors to the spectrum and need to be measured with improved accuracy is critical because of the large number of decays involved. Fortunately, the problem becomes tractable since a limited number of β decays dominate the spectrum [17–19]. The measurement of the decays of these key nuclei has a significant impact on summation calculations. In addition, the dominance of a few decay branches opens up the interesting possibility of performing reactor antineutrino spectroscopy [20], which can only be exploited if it is based on reliable nuclear data. In this context, total absorption γ-ray spectroscopy (TAGS) measurements of the β decays of interest are of great relevance, as was demonstrated in the pioneering work of Ref. [21]. The TAGS technique is based on the use of large scintillator crystals covering a solid angle of almost 4π in order to maximize the detection efficiency and avoid the effect of Pandemonium. This technique has already shown the potential to improve antineutrino spectrum summation calculations [18,21–25].

In this Letter we present a TAGS study of the β decays of the ground states (gs) and metastable states (m) of ^{100}Nb and ^{102}Nb, identified as high-priority contributors to the reactor antineutrino spectrum [18]. The decays of ^{92}Rb, ^{96gs}Y, ^{100gs}Nb, and ^{142}Cs are considered to be the most important contributors in the region of the shape distortion [18]. ^{100gs}Nb exhausts by itself 4.4% of the antineutrino flux emitted by a PWR between 3 and 6 MeV, while the contributions of ^{92}Rb, ^{96gs}Y, and ^{142}Cs add up to 9.9% in the same energy range. The present work provides the first TAGS data for the decay of ^{100gs}Nb, thus giving a complete picture of the impact of these decays, since the other three were recently measured with the TAGS technique [18,23]. The decay of ^{100gs}Nb, as the other three presented here, had remained unmeasured because of the difficulties in its production that are outlined below. ^{102gs}Nb is also a relevant contributor, since it exhausts ~3.5% of the antineutrino global flux of a PWR between 4 and 6 MeV.

The study of these decays is challenging for a number of reasons: (i) the refractory nature of the element Nb, (ii) the existence of metastable states at low excitation energies (313 and 94 keV in ^{100}Nb and ^{102}Nb, respectively [26]), and (iii) the small half-life difference between the pairs of decaying states (1.5 and 2.99 s for ^{100gs,100m}Nb [27], 4.3 and 1.3 s for ^{102gs,102m}Nb [28]). For all these reasons, the present study was performed at the IGISOL IV facility [29] (Jyväskylä, Finland). In this facility refractory elements can be extracted using the ion guide technique. In addition, the available double Penning trap system JYFLTRAP [30] can be used to deliver radioactive beams of very high isotopic purity, which is particularly relevant for TAGS studies. This combination of techniques has been successfully used in previous TAGS experiments for reactor applications [18,22,25,31].

In the experiment we used the new decay total absorption γ-ray spectrometer (DTAS) [32,33]. This detector consists of an array of 18 NaI(Tl) crystals of 15 cm × 15 cm × 25 cm. The nuclei of interest were produced using a proton beam of 25 MeV impinging on a natural uranium target. Following extraction from the fission ion gas cell, ions were guided to the IGISOL separator, accelerated to a potential of 30 kV and mass separated with a modest resolving power. After cooling and bunching [34], high-resolution mass separation of the radioactive beam was achieved using JYFLTRAP. The ions extracted from the trap were implanted in a magnetic tape placed at the center of the DTAS spectrometer, in front of a plastic β detector of 3 mm thickness with a β-detection efficiency of about 30%. The setup included a HPGe detector, placed behind the β detector, to monitor the purity of the beam. During the measurements, a tape transport system served to carry away spent activity, and its collection cycles were selected according to the half-lives of the decays of interest.

The total sum energy was reconstructed off-line from the signals in the individual modules, with the requirement of a coincidence between DTAS and the β detector. The coincidence requirement provided a spectrum free from environmental background, but in the analysis additional sources of contamination had to be taken into account. The summing-pileup distortion was calculated as in previous works [18,22,25], with a Monte Carlo (MC) procedure based on the random superposition of two stored events within the ADC gate length [35,36]. Several calibration sources (^{22,24}Na, ^{60}Co, ^{137}Cs, and ^{152}Eu-^{133}Ba) were used to obtain the energy and resolution calibration of the spectrometer.

In the TAGS analyses we followed the method developed by the Valencia group [37–39]. To determine the β-intensity distribution, one must solve the inverse problem $d_i = \sum_j^{\text{levels}} R_{ij}(B) f_j$ [38], where d_i is the number of

counts in channel i of the spectrum free of contaminants, f_j represents the number of events that feed level j in the daughter nucleus, and R_{ij} is the response function of the detector, which depends on the branching ratios (B) for different deexcitation paths of the states populated in the decay. The branching-ratio matrices for the present Nb decays were calculated using the known level schemes of the daughter nuclei at low excitation energies [27,28]. From the last accepted level up to the Q_β value, a continuum region of 40 keV bins was defined with branching ratios calculated on the basis of the statistical model [39], and modified during the analysis to reproduce a number of observables such as the total energy spectrum with and without different module-multiplicity conditions, the individual crystal spectra and the absolute γ intensities deexciting levels in the known part of the level scheme. The parameters used for the statistical model calculation for each of the analyzed cases were taken from the RIPL-3 database [40]. Once each branching-ratio matrix B was defined, R_{ij} was calculated by means of MC simulations [37] using the GEANT4 simulation package [41]. The MC simulations were validated by comparison with measurements of calibration sources performed during the experiment [36].

Similar strategies were adopted for the $A = 100$ and $A = 102$ systems in order to distinguish experimentally between the decays of the two isomers. The 1^+ ^{100gs}Nb and ^{102m}Nb low-spin isomers were populated selectively through the β decay of the 0^+ ground states of the Zr parents, by extracting ^{100}Zr and ^{102}Zr ions, respectively, from JYFLTRAP. Thus, the decays of the parent Zr isotopes were considered as contaminants in these measurements. In contrast, the high spin isomers, ^{100m}Nb (assumed to be a 5^+ [42]) and ^{102gs}Nb (assumed to be a 4^+), were obtained by selecting the ^{100}Nb and ^{102}Nb ions in the trap. In both cases, the high-spin component was favored in the proton-induced fission process, and the low-spin component was treated as a contaminant that represented 9.4% of the total spectrum of ^{100}Nb and 19.7% in the ^{102}Nb case. The normalization factors of the contaminants of each measurement will be discussed later. In addition, to check the overall consistency of the separation of the isomers, in the ^{100}Nb case we also dedicated a run to collecting data using the Ramsey cleaning purification technique in the trap [43], with higher mass resolving power than the conventional technique.

As a first step we extracted the TAGS spectra from the decay of the low spin Nb isomers, produced in the decay of the Zr parents. If the Zr decays were well known, they could be simulated and subtracted. However, the information available for these decays is incomplete. The Q_β of the decay of ^{100}Zr is 3.421 MeV and the last level populated in β decay seen experimentally is at 704.1 keV [44]. The decay of ^{102}Zr has $Q_\beta = 4.717$ MeV and the highest level populated in β decay seen experimentally is at an excitation energy of 940.5 keV [44]. The time information registered within each measurement cycle allowed us to sort the data for ^{100}Zr + ^{100gs}Nb and ^{102}Zr + ^{102m}Nb off-line using different time windows to exploit the small differences in the half-lives of the implanted (Zr) and daughter (Nb) decays (7.1–1.5 s and 2.9–1.3 s, respectively). Their individual contributions to the combined spectra were obtained by solving linear equations for the content of each bin in the TAGS spectrum. For every time window the weight of each decay was obtained by solving Bateman equations. Using this procedure, we were able to separate the contributions of the spectra of the decays of ^{100}Zr and ^{102}Zr in each of the Zr + Nb combined measurements. Although the extracted spectra exhibited large statistical fluctuations (reaching 100% of the bin content at 2 and 3 MeV, respectively), they allowed us to perform a TAGS analysis to obtain information about the β intensities for the Zr decays. From this analysis we found an additional $< 2\%$ β intensity to a level at 1.26 MeV in ^{100}Nb in the decay of ^{100}Zr. This level had been identified in a reaction study [45], but had not been seen previously in β decay. In the decay of ^{102}Zr 14.5% of the β intensity was seen to populate levels above 940.5 keV and below 3 MeV. In order to avoid the problems related to the statistical fluctuations in the extracted Zr components, we used the smooth spectra obtained from MC simulation as a contaminant in the analyses of the low spin Nb isomers. For this, the β-intensity distributions obtained in the TAGS analyses of the Zr spectra were used as input for the DECAYGEN event generator [39]. The normalization of the decay of ^{100}Zr for the analysis of ^{100gs}Nb was obtained using its most intense γ ray, which connects the level at 400.5 keV with the ground state. Similarly, in the case of ^{102m}Nb the normalization of the decay of ^{102}Zr was obtained from the 599.48 and 535.13 keV γ rays, emitted in the deexcitation of the level at 599.48 keV. The upper panel of Fig. 1 shows the ^{100}Zr contamination obtained in this way. The analysis of the total TAGS spectrum then provides the β intensity for the decay of ^{100gs}Nb.

Once the low-spin decay components were determined in this way, we proceeded to the analyses of the measurements with the mixed contributions from both isomers. Each low-spin Nb spectrum was treated as a contaminant in order to extract the contribution of the high-spin isomer. In the decay of ^{100m}Nb, represented in the lower panel of Fig. 1, the contribution of the low-spin isomeric branch to the spectrum was normalized using the peak at 695.2 keV, associated with a 0^+ level populated only in the decay of the low-spin isomer. Similarly, in the ^{102gs}Nb case the peak associated with the 0^+ state at 698.26 keV, only populated in the decay of ^{102m}Nb, was used in the normalization.

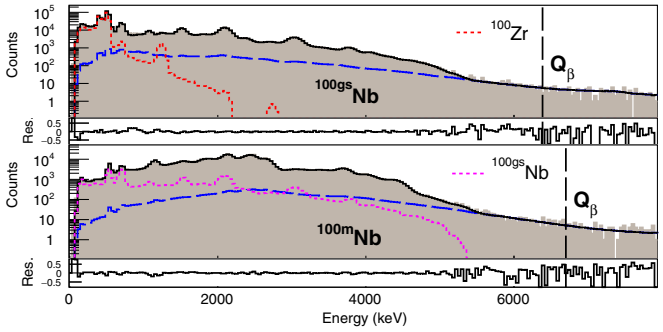

FIG. 1. Relevant histograms for the analyses of ^{100gs}Nb (top) and ^{100m}Nb (bottom): experimental β-gated spectra (gray filled area), summing-pileup (dashed blue line) and reconstructed spectrum (solid black line), which is obtained by the convolution of the response function with the final accepted β-intensity distribution. The corresponding decays of the parent (dotted red line) and the low spin isomer (dotted pink line) are also shown. The relative deviations between experimental and reconstructed spectra are shown below each case.

The quality of the reproduction of the measured and reconstructed spectra for the decays of ^{100gs,100m}Nb is shown in Fig. 1. The β-intensity distributions determined in these analyses are presented in Fig. 2. Several sources of systematic error (statistical errors are negligible in comparison) were considered in the evaluation of the uncertainties, in line with Refs. [22,25,31,46]. The β intensities obtained from high-resolution measurements are also presented, showing that both cases suffered from the Pandemonium effect. In the case of the ^{100gs}Nb 4.4% of the β intensity was found above the last populated level previously known at 3.129 MeV, while for ^{100m}Nb 14.5% of the β intensity feeds levels above 3.65 MeV, the last populated level known from high-resolution measurements. In the $A = 102$ cases (see figures in the Supplemental Material [47]), for ^{102gs}Nb almost 50% of the β intensity was found to populate levels above 2.48 MeV, the highest energy level known to be populated from high-resolution measurements. In the case of ^{102m}Nb no previous β-intensity data were available.

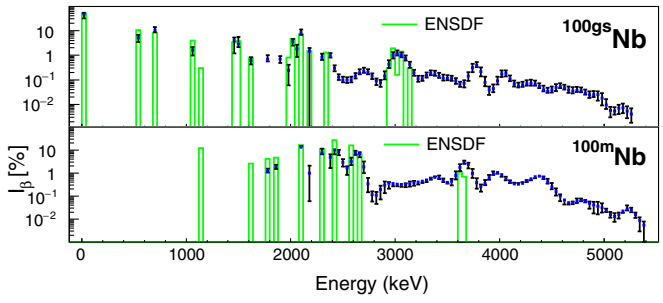

FIG. 2. β-intensity distributions for the decays of ^{100gs}Nb (top) and ^{100m}Nb (bottom): TAGS results (dots with error bars) and high-resolution γ-spectroscopy data from ENSDF (bars).

Antineutrino spectrum calculations have been performed using the summation method developed by the Nantes group [21]. Allowed shapes were assumed for the present cases, since allowed transitions dominate according to the spin-parity values. Figure 3 shows the ratio between the antineutrino spectrum calculated with the inclusion of the present TAGS β-intensity distributions, and the original calculation based on previous knowledge from high resolution measurements for each of the four main fissile isotopes in a PWR reactor. The data for the original calculation came from JEFF-3.1 [48], except for ^{102gs}Nb where they were taken from ENSDF [49]. The impact of the present results is significant in the energy region of the reactor antineutrino shape distortion, especially for the Pu isotopes, with large peaks around 4.5 and 6.5 MeV. Although the new data for ^{100gs,100m}Nb decays have a maximum impact of $\sim$1% for the four fissile isotopes relative to previous high-resolution measurements, the impact of the ^{102}Nb cases is remarkable due to the scarce previous information. The results for ^{102gs}Nb lower the ratio for uranium and plutonium isotopes by up to 3% and 4%, respectively. The ^{102m}Nb results raise the ratio by up to 1%, 2%, 4%, and 6% for ^{238}U, ^{235}U, ^{241}Pu, and ^{239}Pu, respectively. For the first time, the impact of the data reduces the discrepancy between the summation calculations and the measured antineutrino spectra in the region of the shape distortion. The combined effect of our new results shows an even larger influence in the region of shape distortion than previous TAGS studies of the most important contributors in this region: the impact of ^{92}Rb was up to 4.5% for ^{235}U [18], while the combined impact of ^{92}Rb, ^{96gs}Y, and ^{142}Cs

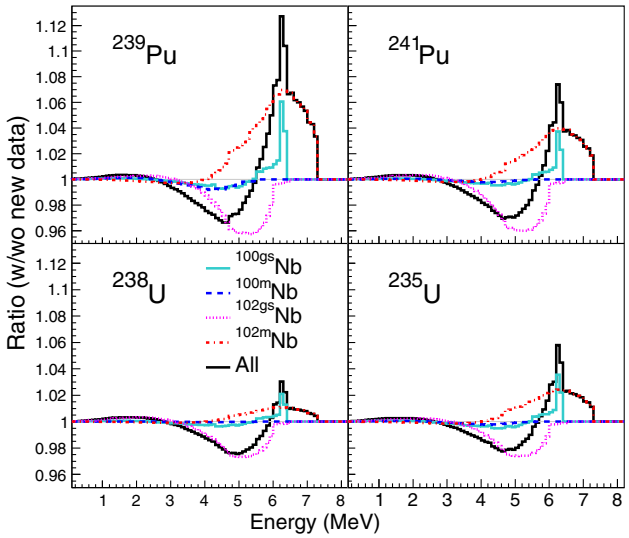

FIG. 3. Ratio of reactor antineutrino spectra as a function of energy when the results obtained in the present work replace the previous knowledge of the decays studied. The spike observed for ^{100gs}Nb is due to a difference in the Q_β value between the original calculation and the current value [26].

amounted to about 3.5% for all fissioning systems in Ref. [23] (with different reference data than were used in Ref. [18]). In the present case the impact is dominated by the ^{102}Nb decay data. This confirms that the final impact can be larger than expected, depending on the missing information in the databases, and on the systematic error introduced by the Pandemonium effect.

Incomplete β-decay data can also lead to an incorrect determination of the decay heat (DH) [31], i.e., the energy released by the decay of fission products in a working reactor and after reactor shut down. The DH as a function of time is estimated using summation calculations, i.e., computed by summing the energy released by each decay (average γ and β energies for β-decaying nuclei) weighted by the corresponding activity. The β-intensity distributions obtained in this work have been used to determine the average γ and β energies released per decay (see average energies in the Supplemental Material [47]).

The impact of the new TAGS data on DH summation calculations has been evaluated and compared with the ENDF/B-VII.1 database [50] used as a reference (due to the lack of previous results for ^{102m}Nb, the estimate $\bar{E}_\gamma = \bar{E}_\beta = Q_\beta/3$ was made). The largest effect is introduced by ^{100gs}Nb and ^{102gs}Nb, where there is an increase of 1% and 1.5% in the ratio of the γ component at 10 s in ^{235}U (1.2% and 1.8%, respectively, in ^{239}Pu). The new results for ^{102m}Nb lower by 1.5% and 3% the γ component in ^{235}U and ^{239}Pu, respectively, below 1 s. The total impact in the β component of ^{235}U and ^{239}Pu at 10 s is a reduction of 1% and 1.3%, respectively.

In conclusion, measurements of the β decay of ^{100gs,100m}Nb and ^{102gs,102m}Nb have been carried out using the TAGS technique. Thanks to the purity of the beams provided by JYFLTRAP and the use of different strategies in the production of the nuclei of interest, we were able to separate the contribution of each isomer in the analyses. Our results show that previous measurements for ^{100gs,100m}Nb and ^{102gs}Nb were affected by the Pandemonium effect, while the β-intensity distribution for ^{102m}Nb has been determined for the very first time. Reactor antineutrino spectrum summation calculations show a large impact of our measurements in the energy region of the shape distortion at 5–7 MeV by up to 2% for ^{235}U and 6% for ^{239}Pu. In addition, an overall increase of around 3% in the DH γ component of ^{235}U and ^{239}Pu was found at 10 s. Both results emphasize the need for TAGS measurements to improve summation calculations for both DH and antineutrino spectrum. Amidst the current debate in the field of antineutrino physics, the latest investigations [51] emphasize the importance of summation calculations in the investigation of the origin of the shape distortion and the flux anomalies. The present results, obtained from very challenging measurements, are a significant step towards improved antineutrino summation calculations and detailed antineutrino spectroscopy of reactors.

This work has been supported by the Spanish Ministerio de Economía y Competitividad under Grants No. FPA2011-24553, No. AIC-A-2011-0696, No. FPA2014-52823-C2-1-P, No. FPA2015-65035-P, No. FPI/BES-2014-068222, and the program Severo Ochoa (SEV-2014-0398), by the Spanish Ministerio de Educación under the FPU12/01527 Grant, by the European Commission under the FP7/EURATOM Contract No. 605203 and the FP7/ENSAR Contract No. 262010, and by the *Junta para la Ampliación de Estudios* Programme (CSIC JAE-Doc contract) co-financed by ESF. V. G. thanks the support of K. Zygmunt. This work was supported by the Academy of Finland under the Finnish Centre of Excellence Programme (Project No. 213503, Nuclear and Accelerator-Based Physics Research at JYFL). It was also supported by the UK Science and Technology Facilities Council (STFC) Grant No. ST/F012012/1.

*Present address: Subatech, IMT-Atlantique, Université de Nantes, CNRS-IN2P3, F-44307, Nantes, France.
guadilla@ific.uv.es
†algora@ific.uv.es

[1] C. L. Cowan, F. Reines, F. B. Harrison, H. W. Kruse, and A. D. McGuire, Science **124**, 103 (1956).
[2] Y. Abe *et al.*, Phys. Rev. Lett. **108**, 131801 (2012).
[3] F. P. An *et al.*, Phys. Rev. Lett. **108**, 171803 (2012).
[4] J. K. Ahn *et al.*, Phys. Rev. Lett. **108**, 191802 (2012).
[5] F. An *et al.*, J. Phys. G **43**, 030401 (2016).
[6] S.-B. Kim, Nucl. Part. Phys. Proc. **265–266**, 93 (2015).
[7] A.A. Hahn, K. Schreckenbach, W. Gelletly, F. von Feilitzsch, G. Colvin, and B. Krusche, Phys. Lett. B **218**, 365 (1989).
[8] N. Haag, A. Gütlein, M. Hofmann, L. Oberauer, W. Potzel, K. Schreckenbach, and F. M. Wagner, Phys. Rev. Lett. **112**, 122501 (2014).
[9] Th. A. Mueller, D. Lhuillier, M. Fallot, A. Letourneau, S. Cormon, M. Fechner, L. Giot, T. Lasserre, J. Martino, G. Mention, A. Porta, and F. Yermia, Phys. Rev. C **83**, 054615 (2011).
[10] P. Huber, Phys. Rev. C **84**, 024617 (2011).
[11] G. Mention, M. Fechner, Th. Lasserre, Th. A. Mueller, D. Lhuillier, M. Cribier, and A. Letourneau, Phys. Rev. D **83**, 073006 (2011).
[12] F. P. An *et al.*, Phys. Rev. Lett. **118**, 251801 (2017).
[13] J. H. Choi *et al.*, Phys. Rev. Lett. **116**, 211801 (2016).
[14] F. P. An *et al.*, Phys. Rev. Lett. **116**, 061801 (2016).
[15] Y. Abe *et al.*, J. High Energy Phys. 01 (2016) 163.
[16] J. C. Hardy, L. C. Carraz, B. Jonson, and P. G. Hansen, Phys. Lett. **71B**, 307 (1977).
[17] A. A. Sonzogni, T. D. Johnson, and E. A. McCutchan, Phys. Rev. C **91**, 011301(R) (2015).
[18] A.-A. Zakari-Issoufou *et al.*, Phys. Rev. Lett. **115**, 102503 (2015).
[19] A. A. Sonzogni, E. A. McCutchan, and A. C. Hayes, Phys. Rev. Lett. **119**, 112501 (2017).
[20] A. A. Sonzogni, M. Nino, and E. A. McCutchan, Phys. Rev. C **98**, 014323 (2018).

[21] M. Fallot, S. Cormon, M. Estienne, A. Algora, V. M. Bui, A. Cucoanes, M. Elnimr, L. Giot, D. Jordan, J. Martino, A. Onillon, A. Porta, G. Pronost, A. Remoto, J. L. Taín, F. Yermia, and A.-A. Zakari-Issoufou, Phys. Rev. Lett. **109**, 202504 (2012).
[22] E. Valencia *et al.*, Phys. Rev. C **95**, 024320 (2017).
[23] B. C. Rasco *et al.*, Phys. Rev. Lett. **117**, 092501 (2016).
[24] A. Fijalkowska *et al.*, Phys. Rev. Lett. **119**, 052503 (2017).
[25] S. Rice *et al.*, Phys. Rev. C **96**, 014320 (2017).
[26] G. Audi, F. G. Kondev, Meng Wang, W.J. Huang, and S. Naimi, Chin. Phys. C **41**, 030001 (2017).
[27] B. Singh, Nucl. Data Sheets **109**, 297 (2008).
[28] D. D. Frenne and E. Jacobs, Nucl. Data Sheets **83**, 535 (1998).
[29] I. D. Moore *et al.*, Nucl. Instrum. Methods Phys. Res., Sect. B **317**, 208 (2013).
[30] T. Eronen *et al.*, Eur. Phys. J. A **48**, 46 (2012).
[31] A. Algora *et al.*, Phys. Rev. Lett. **105**, 202501 (2010).
[32] J. L. Tain *et al.*, Nucl. Instrum. Methods Phys. Res., Sect. A **803**, 36 (2015).
[33] V. Guadilla *et al.*, Nucl. Instrum. Methods Phys. Res., Sect. B **376**, 334 (2016).
[34] A. Nieminen *et al.*, Nucl. Instrum. Methods Phys. Res., Sect. B **204**, 563 (2003).
[35] D. Cano-Ott, J. L. Tain, A. Gadea, B. Rubio, L. Batist, M. Karny, and E. Roeckl, Nucl. Instrum. Methods Phys. Res., Sect. A **430**, 488 (1999).
[36] V. Guadilla *et al.*, Nucl. Instrum. Methods Phys. Res., Sect. A **910**, 79 (2018).
[37] D. Cano-Ott, J. L. Tain, A. Gadea, B. Rubio, L. Batist, M. Karny, and E. Roeckl, Nucl. Instrum. Methods Phys. Res., Sect. A **430**, 333 (1999).
[38] J. L. Tain and D. Cano-Ott, Nucl. Instrum. Methods Phys. Res., Sect. A **571**, 728 (2007).
[39] J. L. Tain and D. Cano-Ott, Nucl. Instrum. Methods Phys. Res., Sect. A **571**, 719 (2007).
[40] R. Capote *et al.*, Nucl. Data Sheets **110**, 3107 (2009).
[41] S. Agostinelli *et al.*, Nucl. Instrum. Methods Phys. Res., Sect. A **506**, 250 (2003).
[42] J. Suhonen and G. Lhersonneau, Phys. Rev. C **64**, 014315 (2001).
[43] T. Eronen, V.-V. Elomaa, U. Hager, J. Hakala, A. Jokinen, A. Kankainen, S. Rahaman, J. Rissanen, C. Weber, and J. Äystö, Nucl. Instrum. Methods Phys. Res., Sect. B **266**, 4527 (2008).
[44] S. Rinta-Antila *et al.*, Eur. Phys. J. A **31**, 1 (2007).
[45] F. Ajzenberg-Selove, E. R. Flynn, D. L. Hanson, and S. Orbesen, Phys. Rev. C **19**, 2068 (1979).
[46] V. Guadilla *et al.*, Phys. Rev. C **96**, 014319 (2017).
[47] See Supplemental Material at http://link.aps.org/supplemental/10.1103/PhysRevLett.122.042502 for $A=102$ figures and average energies.
[48] The JEFF nuclear data library, http://www.oecdnea.org/dbdata/jeff/.
[49] ENSDF database, http://www.nndc.bnl.gov/ensdf.
[50] M. B. Chadwick *et al.*, Nucl. Data Sheets **112**, 2887 (2011).
[51] A. C. Hayes, G. Jungman, E. A. McCutchan, A. A. Sonzogni, G. T. Garvey, and X. B. Wang, Phys. Rev. Lett. **120**, 022503 (2018).